JACS
JOURNAL OF THE AMERICAN CHEMICAL SOCIETY
Communication
pubs.acs.org/JACS

Chloride-Promoted Formation of a Bimetallic Nanocluster $Au_{80}Ag_{30}$ and the Total Structure Determination

Jiu-Lian Zeng,[†] Zong-Jie Guan,[†] Yang Du,[†] Zi-Ang Nan,[†] Yu-Mei Lin,*[,†] and Quan-Ming Wang*[,†,‡]

[†]Department of Chemistry, College of Chemistry and Chemical Engineering, Xiamen University, Xiamen, 361005, PR China
[‡]Department of Chemistry, Tsinghua University, Beijing, 100084, PR China

Supporting Information

ABSTRACT: We report the total structure determination of a large bimetallic nanocluster with an overall composition of $[Au_{80}Ag_{30}(C{\equiv}CPh)_{42}Cl_9]Cl$. It is the largest structurally characterized bimetallic coinage nanocluster so far. The 110 metal atoms are distributed in a concentric four-shell Russian doll arrangement, Au_6@Au_{35}@$Ag_{30}Au_{18}$@Au_{21}. There are 42 PhC≡C— ligands and 9 μ_2-chloride ligands clamping on the cluster surface. The chloride is proven to be critical for the formation of this giant cluster, as the control experiment in the absence of halide gives only smaller species. This work demonstrates that the halide can play a key role in the formation of a large metal nanocluster, and the halide effect should be considered in the design and synthesis of metal nanoclusters.

The determination of structural ordering at the atomic level of metal nanocluster is of extreme significance for fundamental studies of nanomaterials.[1−4] A number of small metal nanoclusters (i.e., Au_{19},[5] Au_{20},[6−8] Au_{23},[9,10] Au_{24},[11−14] Au_{25},[15] Au_{28},[16,17] Au_{30},[18] Au_{36},[19−22] and Au_{38}[23−25]) have been isolated and structurally characterized by X-ray single-crystal diffraction. Large nanoclusters are considered as transitional species from small nanoclusters toward nanoparticles. However, it is still a big challenge to achieve total structural determination of very large nanoclusters. Since the first report of the Au_{102}(p-MBA)$_{44}$ structure in 2007,[26] only two large structures with metal atom number larger than 100 have be resolved, i.e., Au_{133}(p-TBBT)$_{52}$ and Au_{130}(p-MBT)$_{50}$.[27−29]

It has been revealed that the surface ligands help stabilizing nanoclusters, and they also influence the sizes and structures of clusters.[16,30] The coordination preference, bulkiness and electronic nature of ligands can have profound effects on the structures and properties of the clusters.[29,31] The bonding characteristics of the Au-thiolate interface have been extensively studied through both experimental and theoretical studies.[13−33] It has been predicted theoretically that small halide ligands, such as Cl, may have similar behavior as thiolate, i.e., linear Cl−Au−Cl motif vs RS-Au-SR staple.[34] It is well-known that halides as coligands participate in the formation of nanoclusters, e.g., $[Au_{39}(PPh_3)_{14}Cl_6]Cl_2$,[35] $[Au_{20}(PPhpy_2)_{10}Cl_4]Cl_2$,[9] $[Au_{25}(PPh_3)_{10}(SR)_5Cl_2]^{2+}$,[36] $[Au_{24}(PPh_3)_{10}(SR)_5X_2]X$, (X = Cl, Br)[37] and $Au_{24}Ag_{20}(SR)_4(PhC{\equiv}C)_{20}Cl_2$.[38] Recently, Zhu et al. reported a chloride-rich nanocluster $Au_{36}(SCH_2Ph\text{-}^tBu)_8Cl_{20}$.[20] All these examples show that chlorides can be important in the protection of gold/silver nanoclusters.

Herein, we report a large bimetallic 110-metal nanocluster protected by both alkynyl and chloride ligands, $[Au_{80}Ag_{30}(C{\equiv}CPh)_{42}Cl_9]Cl$ (**$Au_{80}Ag_{30}$** for short hereafter). It is the largest structurally characterized bimetallic coinage nanocluster so far. In addition to be a protective ligand, the halide favors the formation of a large cluster over smaller species as proved by control experiments.

The synthesis of **$Au_{80}Ag_{30}$** involves the direct reduction of PhC≡CAu and AgCl. Typically, a freshly prepared solution of $NaBH_4$ was added dropwise to a dichloromethane suspension containing PhC≡CAu and AgCl under vigorous stirring, which was followed by addition of trimethyl amine. The color changed from orange to pale brown and finally dark brown. Then a methanol solution of $AgSbF_6$ was added to the mixture. The reaction continued for 15 h at room temperature in the dark. Then the solvents were removed by rotary evaporation, and the obtained products were redissolved in dichloromethane for crystallization. Black rod crystals of **$Au_{80}Ag_{30}$** were obtained via solvent evaporation.

Single-crystal X-ray crystallography revealed that **$Au_{80}Ag_{30}$** crystallized in centrosymmetric $P\bar{3}1c$ space group. The cluster consists of a monocationic $[Au_{80}Ag_{30}(C{\equiv}CPh)_{42}Cl_9]^+$ and one chloride counterion (Figure 1). The cluster $[Au_{80}Ag_{30}(C{\equiv}CPh)_{42}Cl_9]^+$ has D_3 symmetry, with one C_3 axis passing through the top and bottom centers and three C_2 axes along the equatorial directions. Although the M_{110} core is chiral, the crystal is a racemic mixture. The metal core is composed of 80 gold atoms and 30 silver atoms, which are distributed in a four-shell Russian doll pattern, i.e., a Au_6@Au_{35}@$Ag_{30}Au_{18}$@Au_{21} architecture. The 110-metal core is protected peripherally by 42 PhC≡C— and 9 chloride ligands.

The $Au_{80}Ag_{30}$ core structure and its anatomy are illustrated in Figure 2. The first inner shell is a distorted Au_6 octahedron (Figure 2b). The Au_6 kernel is wrapped by a second shell containing 35 gold atoms. These 35 gold atoms can be divided into three parts. The top and bottom parts are identical, and each has 13-gold-atom in the arrangement of three fused capped pentagonal Au_5. There are nine Au atoms around the waist connecting these two Au_{13} parts to form a tubby cage (Figure 2c). The average Au−Au distance in the second Au_{35} shell is 2.883 Å, which are comparable with the Au−Au distance (2.884 Å) in bulk face-centered cubic Au. The Au−Au distances

Received: April 30, 2016
Published: June 10, 2016

DOI: 10.1021/jacs.6b04471
J. Am. Chem. Soc. 2016, 138, 7848−7851

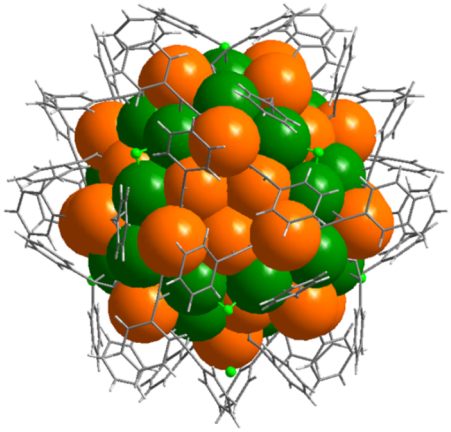

Figure 1. Top view along the C_3 axis of $[Au_{80}Ag_{30}(C{\equiv}CPh)_{42}Cl_9]Cl$. Color codes: orange, Au; dark green, Ag; light green, Cl; gray, C; light gray, H.

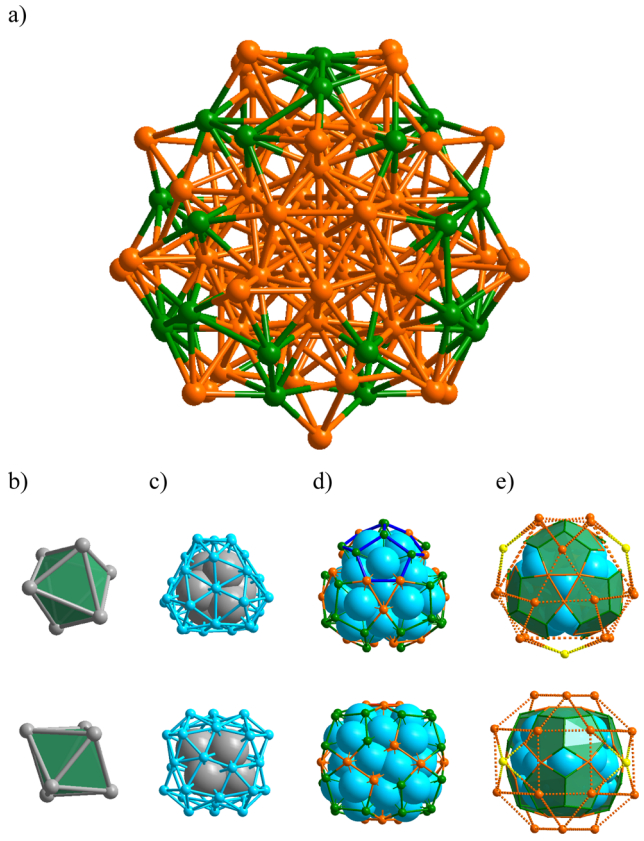

Figure 2. (a) The whole core structure of $Au_{80}Ag_{30}$; top and side views of each shell: (b) Au_6 shell; (c) $Au_6@Au_{35}$ shell; (d) $Au_6@Au_{35}@Ag_{30}Au_{18}$ shell, the M_{10} trefoil structure is highlighted with blue bonds; (e) $Au_6@Au_{35}@Ag_{30}Au_{18}@Au_{21}$ shell. Color codes: orange, gray, sky blue, yellow, Au; dark green, Ag.

between the first shell and the second shell are averaged at 2.852 Å, indicating a compact interaction in these two core–shells. Actually, another description is that these gold atoms are packed based on the interpenetrated icosahedral pattern.

The third shell is a Au–Ag bimetallic shell, which consists of 18 Au atoms and 30 Ag atoms (Figure 2d). The shell is constructed by 18 pentagonal M_5 units divided into six subunits. Three pentagonal M_5 facets join together through edge sharing to from a trefoil structure M_{10} (blue bonds in Figure 2d). Six trefoils are connected through Au vertex sharing to construct a spherical cage, thus there are 18 pentagons in this shell. The average M–M distance in the $Au_{18}Ag_{30}$ core is 3.061 Å. The M–M distances between the second shell (Au_{35}) and the third bimetallic shell ($Ag_{30}Au_{18}$) are averaged at 2.896 Å. In the reported concentric multishell structures of Ag–Au alloy nanoclusters, each shell is always composed of homometals (Ag or Au), e.g., two-shell $Au_{12}@Ag_{20}$ in $Au_{12}Ag_{32}$,[39] three-shell $Au_{12}@Ag_{20}@Au_{12}$ in $Au_{24}Ag_{20}$,[38] three-shell $Ag_2@Au_{18}@Ag_{20}$ in $Ag_{46}Au_{24}$,[40] and four-shell $Ag@Au_{17}@Ag_{27}@Au_{17}$ in $Au_{34}Ag_{28}$.[41] In present work, it is interesting that an inner alloy shell is found in $[Au_{80}Ag_{30}(C{\equiv}CPh)_{42}Cl_9]^+$.

The fourth shell consists of 21 gold atoms. Eighteen of them each caps a pentagonal M_5 face of the third shell. These 18 Au atoms are arranged in an elongated triangular orthobicupola form, which belongs to Johnson solid J_{35} constructed by eight triangles and 12 squares. The remaining three Au atoms are located above the centers of three squares on the C_2 axes (yellow atoms in Figure 2e).

There are 42 PhC≡C— ligands on the surface. Each gold atom of the 21 in the fourth shell is linearly bound by two alkynyl ligands to form a monomeric staple motif (PhC≡C—Au—C≡CPh), and these staples are connected to the metal atoms of subshell with Au-M (M = Ag, Au) bond lengths in the range of 2.881–3.269 Å. As shown in Figure 3, the 21 surface

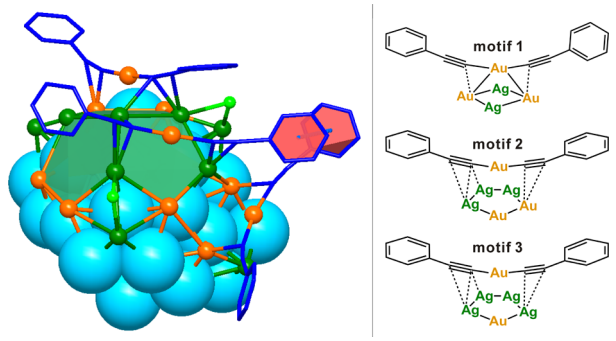

Figure 3. M_2 bridging chlorides (bright green atoms) on surface and three different staple motifs of alkynyl ligands. Color codes: orange, sky blue, Au; dark green, Ag; light green, Cl; blue, C.

monomeric staples are connected to three different types of M_n faces in the subshell, i.e., three staples on Ag_2Au_2 faces (motif 1), 12 on Ag_3Au_2 faces (motif 2), and six on Ag_4Au faces (motif 3). It should be noted that the staples in motif 2 and 3 are linearly and symmetric, while the two benzene rings in motif 1 are arranged in a staggered pattern, allowing for the formation of $\pi{\cdots}\pi$ interactions between the benzene rings of adjacent staple motifs (highlighted in red hexageons in Figure 3 left). Six $\pi{\cdots}\pi$ interactions are observed in $\mathbf{Au_{80}Ag_{30}}$, which enhance the surface attachment of ligands. The 42 PhC≡C– ligands exhibit various coordination modes, six μ_2-η^1(Au),η^1(Au); 12 μ_2-η^1(Au),η^2(Au); six μ_2-η^1(Au), η^2(Ag) and 18 μ_3-η^1(Au),η^1(Ag),η^2(Ag). It is also be noted that the interfacial binding of PhC≡C—Au—C≡CPh motif on the Au(111) surface and the Au_{20} cluster was theoretically found to be energetically preferred.[42] Similar motifs are observed in $\mathbf{Au_{80}Ag_{30}}$. The formation of these different motifs is probably due to steric factors.

Besides 42 PhC≡C— ligands, there are 9 chloride ligands on the surface. All these chlorides are coordinated to Ag atoms of the third shell. Each chloride bridges two Ag atoms of

DOI: 10.1021/jacs.6b04471
J. Am. Chem. Soc. 2016, 138, 7848–7851

adjacent trefoil M_{10}. There are three chlorides on the top and another three at the bottom, and the remaining three chlorides bridge the adjacent Ag atoms of Au_2Ag_2 square in the waist. The Ag−Cl bond lengths are in the range from 2.530 to 2.555 Å. It has been found that chlorides prefer to bind silver atoms other than gold atoms in Au/Ag bimetallic nanocluster, such as in $Au_{24}Ag_{20}$,[38] Ag_xAu_{25-x} nanoclusters.[43]

The important role of chloride has been confirmed by carrying out control experiments monitored by mass spectrometry. **$Au_{80}Ag_{30}$** has a dominant broad peak at 23.4 kDa in MALDI-MS, corresponding to the monocationic ion $[Au_{80}Ag_{30}(C{\equiv}CPh)_{42}Cl_9]^+$ (expected m/z = 23 560) (Figure 4A). However, in the absence of chloride source, the

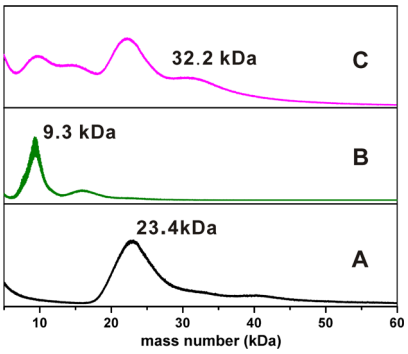

Figure 4. MALDI mass spectra in positive-ion mode of **$Au_{80}Ag_{30}$** and the crude products of control experiments. (A) **$Au_{80}Ag_{30}$**; (B) crude product from the reaction involving no chloride; (C) crude product from the reaction containing NH_4Cl as the chloride source.

preparation under similar reaction conditions led to the formation of a major product with mass peak around 9.3 kDa and no peak from **$Au_{80}Ag_{30}$** was observed (Figure 4B). The reduction of PhC≡CAu and $AgSbF_6$ by $NaBH_4$ in ethanol in the presence of NH_4Cl, **$Au_{80}Ag_{30}$** can be detected and an even larger species at about 32.0 kDa was also generated (Figure 4C). These results indicate that the chloride help stabilize larger clusters. It should be also noted that an analogous bromide cluster $[Au_{80}Ag_{30}(C{\equiv}CPh)_{42}Br_9]Br$ (measured at 23.8 kDa, expected m/z = 23 960) can be obtained when AgCl was replaced by AgBr in the synthesis (Figure S1). The composition of $[Au_{80}Ag_{30}(C{\equiv}CPh)_{42}Br_9]Br$ is also confirmed by EDX measurement, the Au, Ag, and Br atomic ratio of 66.4:24.5:9.1 is close to the calculated value 66.7:25.0:8.3 (Figure. S2).

It can be concluded from the above fact that the critical role of the chloride can be 4-fold: (a) it can be a counteranion for charge balance; (b) it can introduce more metal atoms into the nanocluster; (c) it forms μ_2-bridges between silver atoms to buttress the metal atom arrangement; (d) it with a small size and a spherical shape is available for fitting the space in between metal atoms and helps stabilize the nanocluster. It is noted that halides are also important in controlling the morphology of gold nanocrystals.[44,45] Small halides play a big role in the formation of nanoclusters and nanocrystals.

The properties of **$Au_{80}Ag_{30}$** in solution were also investigated. The UV−vis absorption spectrum of **$Au_{80}Ag_{30}$** in CH_2Cl_2 exhibits four relatively weak absorption bands at 655, 570, 460, and 406 nm (Figure 5). Its bromide analogue shows nearly identical absorption profile. The **$Au_{80}Ag_{30}$** is quite stable even in solution. It is confirmed by UV−vis spectra that no decomposition of **$Au_{80}Ag_{30}$** was observed after its solution had

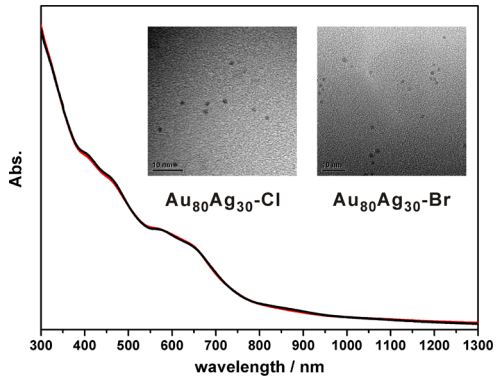

Figure 5. UV−vis spectra of $[Au_{80}Ag_{30}(C{\equiv}CPh)_{42}X_9]X$ (X = Cl, black line, X = Br, red line) in CH_2Cl_2 solution and their TEM images.

been stored under ambient conditions for at least 3 weeks (Figure S3). Furthermore, TEM images show that the nanoclusters particles are uniform with nearly identical sizes at about 1.5 nm, comparable to the size determined by single X-ray crystal structural analysis, suggesting they maintain nanosized structures in solution (Figure 5, inset). This high stability can be understood based on the electron counting. The total number of valence electrons of $[Au_{80}Ag_{30}(C{\equiv}CPh)_{42}Cl_9]^+$ is calculated to be 58 (n = 110 − 42 − 9 − 1), which belongs to the superatomic series.[5,41,46]

In summary, we have synthesized a bimetallic $Au_{80}Ag_{30}$ nanocluster protected by mixed ligands of alkynyl and chloride. It represents the largest bimetallic coinage metal nanocluster so far. The 110 metal atoms in this nanocluster distributed in a concentric four-shell Russian doll arrangement, $Au_6@Au_{35}@Ag_{30}Au_{18}@Au_{21}$. In addition to the surface ligation of 42 phenylalkynyl ligands, nine chlorides bridge the silver atoms. Mass spectrometry analysis indicates that the introduction of small spherical halides favors the formation of larger metal clusters, which demonstrates that halide can be more than a counteranion. The critical effect of halides should be considered in the design and synthesis of metal nanoclusters.

■ ASSOCIATED CONTENT

Supporting Information

The Supporting Information is available free of charge on the ACS Publications website at DOI: 10.1021/jacs.6b04471.

Details of the synthesis, crystallization, X-ray analysis, and supporting figures. (PDF)

Crystallographic data. (CIF)

■ AUTHOR INFORMATION

Corresponding Authors

*linyum@xmu.edu.cn

*qmwang@xmu.edu.cn

Notes

The authors declare no competing financial interest.

■ ACKNOWLEDGMENTS

Dedicated to Prof. T. C. W. Mak on the occasion of his 80th birthday. This work was supported by the 973 Program (2014CB845603) and the Natural Science Foundation of China (21301145, 21473139, 20720150038 and 21521091).

DOI: 10.1021/jacs.6b04471
J. Am. Chem. Soc. 2016, 138, 7848−7851

REFERENCES

(1) Yamazoe, S.; Koyasu, K.; Tsukuda, T. *Acc. Chem. Res.* **2014**, *47*, 816.
(2) Schmid, G. *Chem. Soc. Rev.* **2008**, *37*, 1909.
(3) Parker, J. F.; Fields-Zinna, C. A.; Murry, R. W. *Acc. Chem. Res.* **2010**, *43*, 1289.
(4) Jin, R. *Nanoscale* **2015**, *7*, 1549.
(5) Wan, X. K.; Tang, Q.; Yuan, S. F.; Jiang, D. E.; Wang, Q. M. *J. Am. Chem. Soc.* **2015**, *137*, 652.
(6) Wan, X. K.; Lin, Z. W.; Wang, Q. M. *J. Am. Chem. Soc.* **2012**, *134*, 14750.
(7) Zeng, C.; Liu, C.; Chen, Y.; Rosi, N. L.; Jin, R. *J. Am. Chem. Soc.* **2014**, *136*, 11922.
(8) Wan, X. K.; Yuan, S. F.; Lin, Z. W.; Wang, Q. M. *Angew. Chem., Int. Ed.* **2014**, *53*, 2923.
(9) Wan, X. K.; Yuan, S. F.; Tang, Q.; Jiang, D. E.; Wang, Q. M. *Angew. Chem., Int. Ed.* **2015**, *54*, 5977.
(10) Das, A.; Li, T.; Nobusada, K.; Zeng, C.; Rosi, N. L.; Jin, R. *J. Am. Chem. Soc.* **2013**, *135*, 18264.
(11) Wan, X. K.; Xu, W. W.; Yuan, S. F.; Gao, Y.; Zeng, X. C.; Wang, Q. M. *Angew. Chem., Int. Ed.* **2015**, *54*, 9683.
(12) Das, A.; Li, T.; Li, G.; Nobusada, K.; Zeng, C.; Rosi, N. L.; Jin, R. *Nanoscale* **2014**, *6*, 6458.
(13) Song, Y.; Wang, S.; Zhang, J.; Kang, X.; Chen, S.; Li, P.; Sheng, H.; Zhu, M. *J. Am. Chem. Soc.* **2014**, *136*, 2963.
(14) Das, A.; Li, T.; Nobusada, K.; Zeng, Q.; Rosi, N. L.; Jin, R. *J. Am. Chem. Soc.* **2012**, *134*, 20286.
(15) Zhu, M.; Aikens, C. M.; Hollander, F. J.; Schatz, G. C.; Jin, R. *J. Am. Chem. Soc.* **2008**, *130*, 5883.
(16) Chen, Y.; Liu, C.; Tang, Q.; Zeng, C.; Higaki, T.; Das, A.; Jiang, D. E.; Rosi, N. L.; Jin, R. *J. Am. Chem. Soc.* **2016**, *138*, 1482.
(17) Zeng, C.; Li, T.; Das, A.; Rosi, N. L.; Jin, R. *J. Am. Chem. Soc.* **2013**, *135*, 10011.
(18) Crasto, D.; Malola, S.; Brosofsky, G.; Dass, A.; Häkkinen, H. *J. Am. Chem. Soc.* **2014**, *136*, 5000.
(19) Zeng, C.; Qian, H.; Li, T.; Li, G.; Rosi, N. L.; Yoon, B.; Barnett, R. N.; Whetten, R. L.; Landman, U.; Jin, R. *Angew. Chem., Int. Ed.* **2012**, *51*, 13114.
(20) Yang, S.; Chai, J.; Song, Y.; Kang, X.; Sheng, H.; Chong, H.; Zhu, M. *J. Am. Chem. Soc.* **2015**, *137*, 10033.
(21) Das, A.; Liu, C.; Zeng, C.; Li, G.; Li, T.; Rosi, N. L.; Jin, R. *J. Phys. Chem. A* **2014**, *118*, 8264.
(22) Nimmala, P. R.; Knoppe, S.; Jupally, V. R.; Delcamp, J. H.; Aikens, C. M.; Dass, A. *J. Phys. Chem. B* **2014**, *118*, 14157.
(23) Liu, C.; Li, T.; Li, G.; Nobusada, K.; Zeng, C.; Pang, G.; Rosi, N. L.; Jin, R. *Angew. Chem., Int. Ed.* **2015**, *54*, 9826.
(24) Qian, H.; Eckenhoff, W. T.; Zhu, Y.; Pintauer, T.; Jin, R. *J. Am. Chem. Soc.* **2010**, *132*, 8280.
(25) Molina, B.; Sanchez-Castillo, A.; Knoppe, S.; Garzon, I. L.; Burgi, T.; Tlahuice-Flores, A. *Nanoscale* **2013**, *5*, 10956.
(26) Jadzinsky, P. D.; Calero, G.; Ackerson, C. J.; Bushnell, D. A.; Kornberg, R. D. *Science* **2007**, *318*, 430.
(27) Zeng, C.; Chen, Y.; Kirschbaum, K.; Appavoo, K.; Sfeir, M. Y.; Jin, R. *Sci. Adv.* **2015**, *1*, e1500045.
(28) Dass, A.; Theivendran, S.; Nimmala, P. R.; Kumara, C.; Jupally, V. R.; Fortunelli, A.; Sementa, L.; Barcaro, G.; Zuo, X.; Noll, B. C. *J. Am. Chem. Soc.* **2015**, *137*, 4610.
(29) Chen, Y.; Zeng, C.; Liu, C.; Kirschbaum, K.; Gayathri, C.; Gil, R. R.; Rosi, N. L.; Jin, R. *J. Am. Chem. Soc.* **2015**, *137*, 10076.
(30) Häkkinen, H. *Nat. Chem.* **2012**, *4*, 443.
(31) Chen, Y.; Zeng, C.; Kauffman, D. R.; Jin, R. *Nano Lett.* **2015**, *15*, 3603.
(32) Jiang, D. E.; Tiago, M. L.; Luo, W.; Dai, S. *J. Am. Chem. Soc.* **2008**, *130*, 2777.
(33) Jiang, D. E. *Nanoscale* **2013**, *5*, 7149.
(34) Jiang, D. E.; Walter, M. *Nanoscale* **2012**, *4*, 4234.
(35) Teo, B. K.; Shi, X.; Zhang, H. *J. Am. Chem. Soc.* **1992**, *114*, 2743.
(36) Qian, H.; Eckenhoff, W. T.; Bier, M. E.; Pintauer, T.; Jin, R. *Inorg. Chem.* **2011**, *50*, 10735.
(37) Das, A.; Li, T.; Nobusada, K.; Zeng, Q.; Rosi, N. L.; Jin, R. *J. Am. Chem. Soc.* **2012**, *134*, 20286.
(38) Wang, Y.; Su, H.; Xu, C.; Li, G.; Gell, L.; Lin, S.; Tang, Z.; Häkkinen, H.; Zheng, N. *J. Am. Chem. Soc.* **2015**, *137*, 4324.
(39) Yang, H.; Wang, Y.; Huang, H.; Gell, L.; Lehtovaara, L.; Malola, S.; Häkkinen, H.; Zheng, N. *Nat. Commun.* **2013**, *4*, 2422.
(40) Wang, S.; Jin, S.; Yang, S.; Chen, S.; Song, Y.; Zhang, J.; Zhu, M. *Sci. Adv.* **2015**, *1*, e1500441.
(41) Wang, Y.; Wan, X. K.; Ren, L.; Su, H.; Li, G.; Malola, S.; Lin, S.; Tang, Z.; Häkkinen, H.; Teo, B. K.; Wang, Q. M.; Zheng, N. *J. Am. Chem. Soc.* **2016**, *138*, 3278.
(42) Tang, Q.; Jiang, D.-E. *J. Phys. Chem. C* **2015**, *119*, 10804.
(43) Wang, S.; Meng, X.; Das, A.; Li, T.; Song, Y.; Cao, T.; Zhu, X.; Zhu, M.; Jin, R. *Angew. Chem., Int. Ed.* **2014**, *53*, 2376.
(44) Zhang, J.; Langille, M. R.; Personick, M. L.; Zhang, K.; Li, S.; Mirkin, C. A. *J. Am. Chem. Soc.* **2010**, *132*, 14012.
(45) Padmos, J. D.; Personick, M. L.; Tang, Q.; Duchesne, P. N.; Jiang, D.-E.; Mirkin, C. A.; Zhang, P. *Nat. Commun.* **2015**, *6*, 7664.
(46) Walter, M.; Akola, J.; Lopez-Acevedo, O.; Jadzinsky, P. D.; Calero, G.; Ackerson, C. J.; Whetten, R. L.; Grönbeck, H.; Häkkinen, H. *Proc. Natl. Acad. Sci. U. S. A.* **2008**, *105*, 9157.

DOI: 10.1021/jacs.6b04471
J. Am. Chem. Soc. 2016, 138, 7848−7851